EMISSION CHARACTERISTICS AND PARAMETERS OF CuInSe$_2$ LASER TORCH PLASMA

M.P. CHUCHMAN, G.E. LASLOV, A.K. SHUAIBOV, L.L. SHIMON

Uzhgorod National University
(46, Pidhirna Str., Uzhgorod 88000, Ukraine; e-mail: shuaibov@univ.uzhgorod.ua)

Radiation spectra and oscillograms of the spectral line intensity of the CuInSe$_2$-based laser erosion plasma are investigated. It is established that the radiation spectra from the hot zone of this laser erosion plasma include spectral lines of excited atoms of copper, indium, and selenium, as well as their singly charged ions. The main parameters and the characteristics of a CuInSe$_2$ laser torch such as the velocity of propagation, ion recombination times, temperature, and concentration of particles are determined. It is shown that, on the initial stages of existence of the plasma, the dominant process is the recombination, whereas, as the distance from a target and the time increase, the gas-dynamic and thermal effects arise. This determines, to a large extent, the peculiarities of the formation of excited atoms and ions.

1. Introduction

CuInSe$_2$ is one of the materials most widely used in the production of high-efficiency solar cells [1, 2]. The maximum efficiency for CuInSe$_2$ was achieved in 2005 and reached 19.3% [3]. Light-sensitive CuInSe$_2$ films are fabricated with the use of a complicated technology, that is why the development of cheaper and easier methods of production of light-sensitive thin layers based on this compound is now of high urgency.

One of the promising techniques of formation of CuInSe$_2$ films is the laser-induced evaporation [4–7]. Properties of thin films obtained in such a way depend on the conditions of evaporation of an initial material, laser radiation parameters, and the substrate temperature. In [8], it was shown that the use of CuIn$_3$Se$_5$ or CuIn$_5$Se$_8$ can improve the radiation stability of light-sensitive films for absorption bands at 0.8–3.5 eV.

The obtained CuInSe$_2$ thin films were characterized by a good substrate adhesion [3]. Investigations of the film structure at various temperatures have demonstrated that, at the temperatures $T = 528$–571 K, the films consist of large (~ 100 nm) oval crystals. With increasing temperature, the area and the height of crystals decrease by a factor of three. Changes in the form and the size of crystals can testify to a variation of both the structure and the composition of CuInSe$_2$ films induced by temperature changes. The growth of the substrate temperature from 720 to 770 K results in the enhancement of the photoelectromotive force by up to three orders of magnitude [3].

This work reports on the results of the emission diagnostics of characteristics and parameters of a multi-component laser torch that can be useful for the spectroscopy, analysis of physico-chemical processes, and optimization of technological processes.

2. Experimental Technique

The experiments were carried out using a repetitively pulsed neodymium laser operating in the Q-switching mode. The radiation pulse duration amounted to 20 ns, while the pulse repetition rate was equal to 12 Hz. The laser radiation was focused with the help of a lens with a focal length of 50 cm. The focusing of the radiation into a spot 0.4–0.5 mm in diameter allowed us to obtain a power density of 5×10^8 W/cm^2 on the target surface. The target represented a CuInSe$_2$ polycrystal. The residual air pressure in the vacuum chamber amounted to 3–12 Pa. The radiation was analyzed with the help of an MDR-2 monochromator with a grating of 1200 l/mm in the spectral region 210–600 nm and a FEU-106 photomultiplier. The radiation was selected from a 0.3-mm-thick region of the laser torch using a lens located at distances of 1 and 7 mm from the target.

The time-averaged spectra were registered with the help of a FEU-106 photomultiplier and a KSP-4 recorder. The FEU-106 system and the MDR-2 monochromator were calibrated with respect to the radiation of hydrogen and tungsten lamps. This allowed us to measure the relative intensities of the radiation lines (I/k_λ, where k_λ is the relative spectral sensitivity of the registration system). Oscillograms of the spectral line intensities of the laser plasma were investigated with the help of an electron linear multiplier ELU-14 FS and a 6-LOR04 oscilloscope. The time resolution amounted to 2–3 ns.
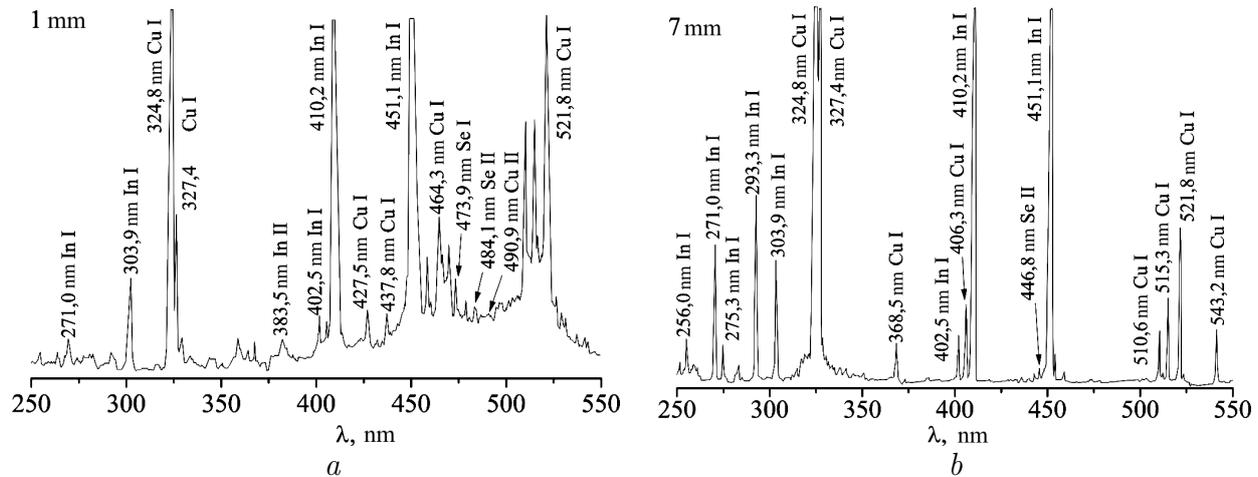
Fig. 1. Radiation spectra of the CuInSe$_2$ laser erosion plasma

3. Results and Their Discussion

Figure 1 shows the radiation spectra of the CuInSe$_2$ erosion plasma. The interpretation of the spectra performed using data given in [9] is presented in Table. It includes the electron configurations, terms, energies of upper excited states, and radiation wavelengths and intensities that were averaged over the time of observation of the plasma radiation formed by one laser pulse and normalized to the maximum intensity of the lines registered at a fixed distance from the target.

We registered the line radiation against the continuous background. The most intense line belonged to indium and had a wavelength of 451.1 nm. If taking its intensity as unity, the maximum intensity for copper was equal to 0.96 at a wavelength of 521.8 nm. As was expected, the most intense were the resonance lines of copper and indium atoms. Spectral lines of copper atoms appear in the whole spectrum (219.9–546.3 nm), whereas those of indium are concentrated in a somewhat narrower spectral range between 227.8 and 487.8 nm. Weak spectral lines of selenium atoms and ions were also registered practically in the whole spectral region under study. The ion component is mainly presented by copper and selenium. A characteristic feature is the presence of spectral ion lines of Se II and the absence of intense ion lines of In II. In the radiation spectrum of the laser plasma based on this compound, one can see the radiation from shifted states of copper atoms. Transitions from such states were best observed in the laser plasma based on pure copper [10].

Among the most intense spectral lines that can be used for the diagnostics of the CuInSe$_2$-based laser torch (the lines whose intensity exceeds 20% of the most intense spectral line), one can mark out the following atomic lines: 324.8, 327.4, 521.8, 515.8, 515.3, 510.6 nm Cu I and 410.2, 451.1 nm In I at a distance of 1 mm from the target; 221.6, 271.0, 324.8, 327.4, 515.3, 521.8, 543.2 nm Cu I and 293.3, 303.9, 410.2, 451.1 nm In I at a distance of 7 mm from the target.

If the upper energy level for a spectral transition of indium atoms exceeds 5 eV, then the radiation intensity at a distance of 7 mm will be lower than that at 1 mm. In the opposite case, the intensity at a distance of 7 mm will be larger. In the case of atomic spectral lines and the increasing distance from the target, the terms of the states producing radiative transitions correspond to lower electron configurations. The majority of spectral lines in the radiation spectrum belongs to copper atoms. More than 60% of them correspond to transitions from shifted states. The intensity of such spectral lines usually does not exceed 10% of the most intense spectral line. At a distance of 1 mm from the target, one registers three spectral lines of selenium atoms, whose upper excited states lie in the energy interval 8.59–8.63 eV. At a distance of 7 mm from the target, the spectral lines of selenium atoms disappear together with those of indium ions. The registered spectral line of indium ion corresponds to an upper energy level of 21.11 eV. For copper ions, we observed spectral lines related to transitions from upper excited states in the energy interval between 16.85 and 17.22 eV. For selenium atoms and ions at 1 mm from the target, there appear spectral lines corresponding to transitions from the energy levels in the interval 14.39–16.26 eV. At the 7-mm distance from the target, one observes spectral lines of selenium ions related to transitions from the still narrower interval of upper state

Interpretation of the radiation spectra of the CuInSe₂ laser plasma

λ, nm	Atom, ion	I_1, rel. un.	I_7, rel. un.	Term$_u$	E_u, eV	λ, nm	Atom, ion	I_1, rel. un.	I_7, rel. un.	Term$_u$	E_u, eV
219.90	Cu I	–	0.17	s4p" $^2D_{3/2}$	7.27	435.40	Cu I	0.03	–	s5s' $^2D_{3/2}$	8.09
221.60	Cu I	–	0.27	s4p" $^2P_{3/2}$	6.98	437.80	Cu I	0.07	0.01	s5s' $^4D_{5/2}$	7.80
227.80	In I	–	0.07	–	5.45	440,10	Se II	0,05	–	–	16,2
252.20	In I	0.03	0.05	7d $^2D_{5/2}$	5.19	441.60	Cu I	0.05	0.01	s5s' $^4D_{3/2}$	7.88
256.00	In I	0.04	0.10	6d $^2D_{3/2}$	4.84	444.60	Se II	0.06	0.02	–	15.05
259.30	Cu I	0.02	0.04	–	–	446.80	Se II	–	0.03	–	15.03
260.20	In I	0.03	–	8s $^2S_{1/2}$	5.03	448.00	Cu I	0.09	–	6s $^2S_{1/2}$	6.55
261.80	Cu I	0.02	0.03	5p $^2P_{3/2}$	6.12	451.10	In I	1.00	1.00	6s $^2S_{1/2}$	3.02
262.70	Cu I	0.02	–	s5d' $^4D_{3/2}$	9.79	454.00	Cu I	–	0.03	s5s' $^4D_{3/2}$	7.88
264.50	Cu I	0.04	–	s5d' $^4D_{5/2}$	9.65	458.70	Cu I	0.18	0.03	s5s' $^4D_{5/2}$	7.80
271.00	In I	0.05	0.26	6d $^2D_{5/2}$	4.84	461.20	In I	0.11	–	–	–
275.30	In I	0.03	0.07	7s $^2S_{1/2}$	4.50	464.30	Cu I	0.27	–	s5s' $^2D_{3/2}$	8.09
277.50	In I	0.03	–	s5p^2 $^4P_{3/2}$	4.46	467.50	Cu I	0.21	–	s5s' $^4D_{5/2}$	7.80
282.40	Cu I	0.03	0.02	s4p' $^2D_{5/2}$	5.77	469.70	Cu I	0.23	–	s5s' $^4D_{3/2}$	7.88
283.70	In I	0.03	0.03	s5p^2 $^4P_{5/2}$	4.64	473.90	Se I	0.17	–	6p $^5P_2$	8.59
293.30	In I	0.04	0.33	7s $^2S_{1/2}$	4.50	474.20	Se I	0.11	–	6p $^5P_1$	8.59
303.90	In I	0.14	0.23	5d $^2D_{3/2}$	4.07	479.40	Cu I	0.14	–	–	8.09
315.70	Cu I	–	0.03	s4p' $^4D_{1/2}$	5.56	481.30	Cu II	0.10	–	4f $^1D_2$	17.1
317.00	Cu I	–	0.05	s4d' $^4G_{7/2}$	9.06	484.10	Se II	0.13	–	5p $^2S^0_{1/2}$	14.5
319.40	Cu I	–	0.06	s4p' $^4D_{3/2}$	5.52	487.80	In I	0.11	–	–	5.56
322.30	Cu I	–	0.05	s4d' $^4F_{3/2}$	9.09	490.96	Cu II	0.12	–	4f $^3H_6$	16.8
324.80	Cu I	0.81	0.98	4p $^2P_{3/2}$	3.81	493.20	Cu II	0.11	–	4f $^3H_5$	16.8
327.40	Cu I	0.21	0.82	4p $^2P_{1/2}$	3.78	495.40	Cu II	0.14	–	4f $^1H_5$	17.1
329.30	Cu I	0.05	0.08	s4d' $^4P_{3/2}$	8.91	497.60	Se II	0.14	–	5p $^2D^0_{5/2}$	14.93
331.70	Cu I	–	0.05	s4d' $^4F_{9/2}$	8.83	499.30	Se II	0.14	–	5p $^4P^0_{3/2}$	14.48
333.50	Cu I	0.03	0.04	s4d' $^2F_{7/2}$	8.81	501.70	Cu I	0.15	–	s5s' $^4D_{1/2}$	7.99
335.40	Cu I	–	0.03	s4d' $^2D_{3/2}$	8.94	503.40	Cu I	0.15	–	s5s' $^4D_{3/2}$	7.88
336.50	Cu I	–	0.03	s4d' $^2G_{9/2}$	8.78	505.20	Cu II	0.16	–	4f $^3G_5$	16.8
337.60	Cu I	–	0.03	s4d' $^4P_{5/2}$	8.82	507.60	Cu I	0.16	–	s5s' $^2D_{5/2}$	8.01
341.30	Cu I	–	0.03	s4d" $^2P_{1/2}$	9.31	510.60	Cu I	0.56	0.15	4p $^2P_{3/2}$	3.81
345.00	Cu I	0.02	–	–	9.37	511.90	Cu I	–	0.03	–	7.99
351.20	Cu I	0.02	0.02	s4d' $^4G_{9/2}$	8.92	515.30	Cu I	0.58	0.25	4d $^2D_{3/2}$	6.19
359.40	Cu I	0.05	–	s4p' $^4P_{5/2}$	4.83	515.80	Cu I	0.31	–	–	8.09
364.50	Cu I	0.03	–	s4d' $^4F_{5/2}$	9.08	517.60	Se II	0.27	–	5p $^4D^0_{5/2}$	14.39
368.50	Cu I	0.04	0.06	–	8.82	521.80	Cu I	0.96	0.45	4d $^2D_{5/2}$	6.19
383.50	In II	0.04	–	–	21.1	522.80	Se II	–	0.03	5p $^4D^0_{7/2}-$	14.6
387.70	Se II	0.02	–	–	15.7	525.40	In I	0.16	–	–	5.38
402.30	Cu I	0.06	0.08	5d $^2D_{3/2}$	6.86	526.30	In I	0.18	–	–	5.38
406.30	Cu I	0.05	0.12	5d $^2D_{5/2}$	6.86	529.30	Cu I	0.14	–	s5s' $^4D_{7/2}$	7.73
410.20	In I	0.69	0.74	6s $^2S_{1/2}$	3.02	531.60	Cu II	0.12	–	5d $^3D_1$	17.2
418.10	Cu II	0.03	–	–	17.5	537.40	Se I	0.09	–	6p $^3P_1$	8.63
423.10	Cu I	0.03	–	s5s" $^2D_{5/2}$	8.32	540.80	Cu I	0.08	–	–	8.02
424.90	Cu I	0.04	–	s5s' $^4D_{1/2}$	7.99	543.20	Cu I	0.07	0.20	s5s' $^4D_{5/2}$	7.80
427.50	Cu I	0.08	–	s5s' $^4D_{7/2}$	7.73	546.30	Cu I	0.04	–	s5s' $^4D_{1/2}$	7.99
432.90	Se I	0.04	–	–	9.18						

energies — 14.6–15.05 eV. Such peculiarities testify to the specific character of the formation of upper excited states of atoms and ions most probably related to the mechanism of atomization of the target, as well as to the manifestation of physico-chemical processes in the laser plasma.
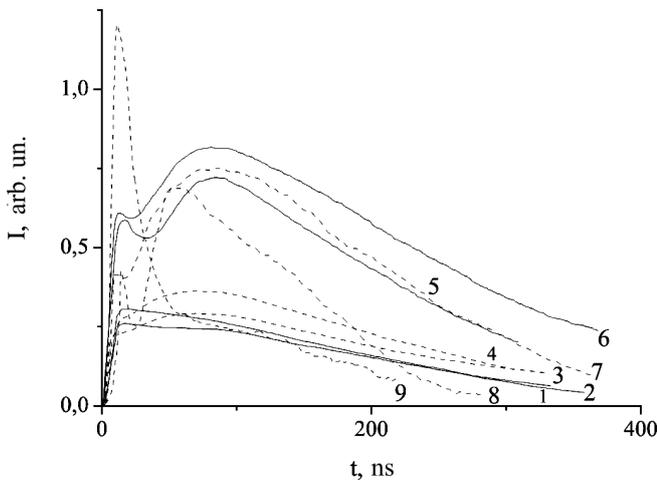
Fig. 2. Radiation oscillograms of the CuInSe$_2$-based laser erosion plasma at 1 mm from the target: *1* -– 521.8 nm Cu I; *2* -– 515.3 nm Cu I; *3* -– 410.2 nm In I; *4* -– 451.1 nm In I; *5* -– 327.4 nm Cu I; *6* -– 324.8 nm Cu I; *7* — 303.9 nm In I; *8* -– 293.3 nm In I; *9* – 271 nm In I

It follows from Fig. 2 that the radiation oscillograms are characterized by two maxima. The first one is registered at 10–14 ns for indium and 13–18 ns for copper, while the second one is observed at 56–85 ns and 82–85 ns, respectively. The use of these data for the estimation of the average velocity of the first maximum for particles of various plasma components yields 83 and 63 km/s for indium and copper, respectively. For the second maximum, the velocities are closer and amount to 14 and 12 km/s for indium and copper, respectively.

Thus, one can conclude that there is more copper at the center of the laser torch and more indium at the periphery. The dispersion of various elements of the multicomponent plasma decreases with time. Here, it is worth noting the influence of gas-dynamic effects and the need for a chemically active or inactive gas in the vacuum chamber. Choosing the pressure of this gas, it is possible to correct the chemical composition of the condensate (with the help of chemical reactions in the gas phase and on the surface), its structure (by changing the energy of moving particles interacting with the external gas), as well as the dispersion of various elements of the plasma [11].

The higher the energy of the upper excited state for a spectral line radiated by an atom, the more pronounced the first maximum of the spectral radiation intensity on the oscillograms (Fig. 2) and the higher its intensity. This effect is equally manifested for copper and indium spectral lines. The radiation time of the spectral lines decreases, as the upper energy level increases. The most

intense radiation in the spectrum was that of copper and indium atoms. It is worth noting that the spectral line of the indium atom has the highest intensity in the first maximum, whereas the spectral line of the copper atom – in the second one. Selenium provides only relatively weak lines in the radiation spectrum, for which we did not manage to obtain clear oscillograms. Their intensity is much lower than the emission intensity of copper or indium atoms.

Judging by the obtained oscillograms, one can conclude that, at the time of appearance of the first maximum, there prevail processes of three-particle recombination, while, at the time of appearance of the second maximum, the dominant role is played by excitations due to collisions with thermal plasma electrons that acquire the energy partially due to the energy transfer in the process of recombination on the initial stages of existence of the plasma [12].

Based on the time of observation of the radiation with regard for the average velocity of the plasma, one can estimate the dimensions of the plasma torch moving through the radiation take-off region. At a distance of 1 mm from the target, the longitudinal dimension of the plasma has an order of 10 mm. Proceeding from the fact the radiation is observed much longer than the time during which the laser acts on the target t_{las}, it is worth noting the considerable expansion of the plasma in the course of its motion at close distances from the target, as well as the possibility that the time of evaporation of the target is longer than t_{las}.

Figure 3 shows the rates of change of the intensity for the spectral lines under study. One can see that the spread of the rates of change of the intensity at transitions from levels with different energies is larger for indium atom than for copper one.

The highest rate of change of the intensity is characteristic of the spectral lines corresponding to transitions from highly excited states of copper and indium atoms. The recombination times for singly charged indium ions obtained from these data amount to 30 ns at observation times of 25–50 ns and 56 ns at observation times close to 200 ns. The recombination time of the corresponding copper ions is much larger (see Fig. 3). It was equal to 139 ns for the time interval 250–300 ns.

Thus, a conclusion can be made that the majority of ionized copper particles coming to the substrate will favor its effective incorporation into the film structure due to a larger mobility provided by the energy of highly excited and ionized particles. This must still stronger smooth the space dispersion of the elements of the target material, because, in the case of indium, the kinetic
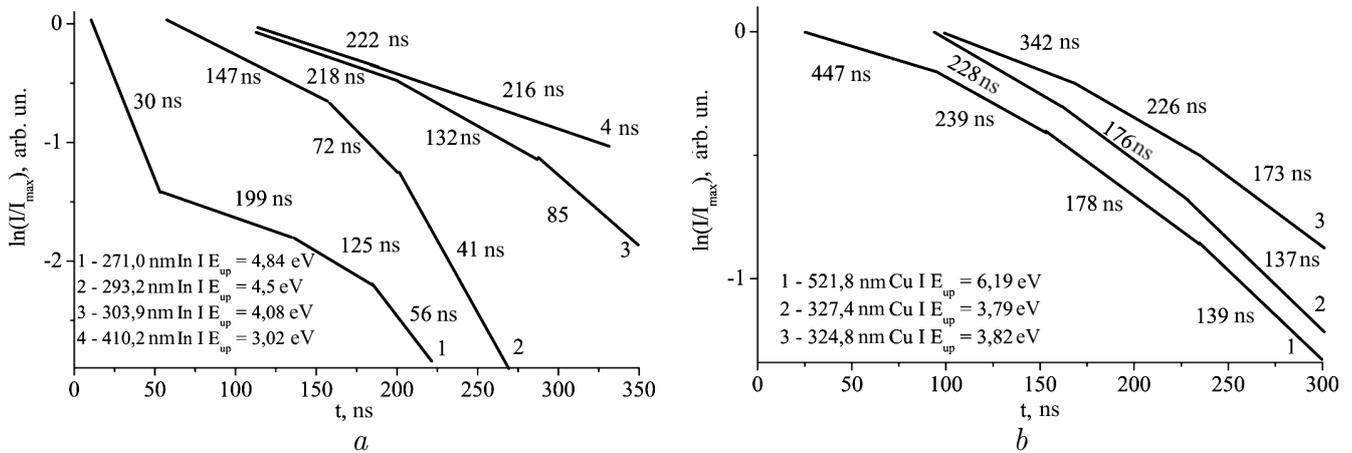
Fig. 3. Rates of change of the spectral radiation intensity of the CuInSe$_2$ laser erosion plasma at 1 mm from the target

energy of moving particles is larger, while the number of ionized particles is smaller. It is due to the appearance of indium at the periphery of the plasma torch, where the temperature and the concentration of electrons are lower. In turn, copper appears closer to the center of the plasma torch, where the temperature is higher. In addition, copper possesses autoionization states in the plasma torch, whose times of thermal and radiative relaxations are much larger than those for nonshifted one-electron excited states. Due to this fact, the populations of such states can significantly exceed, with time, those of non-shifted excited states with one-electron excitation.

As follows from Fig. 3, the efficiency of formation of lower excited states of indium atoms grows. At times of 100–200 ns, the rate of change of the intensity at transitions from low-energy states is larger in indium, whereas at 200–300 ns, – it is higher in copper. This testifies to the domination of the recombination processes of excitation at the leading edge of the plasma and excitation due to collisions with free electrons at its trailing edge. This also leads to a redistribution of the excitation energy between particles of different kinds in the laser torch.

According to Fig. 4, the variation of the distance from 1 to 7 mm results in the insignificant change of the electron temperature (from 0.7 to 0.8 eV). The growth of the temperature at the plasma expansion can be explained by the effect of the expansion gas dynamics on the plasma parameters. At close distances, the plasma expands, whereas at larger ones, it will be gradually compressed due to the accumulation of particles in the vicinity of the shock-wave leading edge that gradually reduces the plasma velocity. That is why the major part of the

material will run after it with time. According to the gas laws, the temperature grows under such conditions.

One can also say that the concentrations of atoms in the ground state differ much stronger than those of ground-state ions. This can be illustrated by comparing the populations of various atoms in Fig. 4 at their ionization energies. The energy introduced to the target is sufficient for the almost complete ionization of the material removed from the target. According to the estimates performed for pure copper and indium, the specific power necessary to completely ionize the target substance under our conditions amounts to 10.7×10^8 and 2.2×10^8 W/cm^2, respectively. This implies that, in spite of the absence of data for selenium and the high probability to find it in the form of complexes due to chemical reactions at the late stages of existence of the plasma, the stoichiometry of a film obtained from the latter must as a whole correspond to the stoichiometry of the target. A more thorough attention must be paid to the area and volume homogeneity of the composition and the film structure. At the initial stages, the plasma will almost completely consist of singly charged ions [11]. Moreover, the dynamics of plasma motion, as well as the specific character of recombination processes, will determine the number of ionized particles that will reach the substrate carrying the additional energy necessary to obtain an ordered film structure. Based on the information about the energy balance of the plasma at the late stages of spread, one make a decision on the necessity of the additional thermal influence on the substrate, where the film is formed, in the case if it is placed at such a distance from the target that the energy carried by fast and ionized particles will be insufficient to form the crystal structure of the film, for
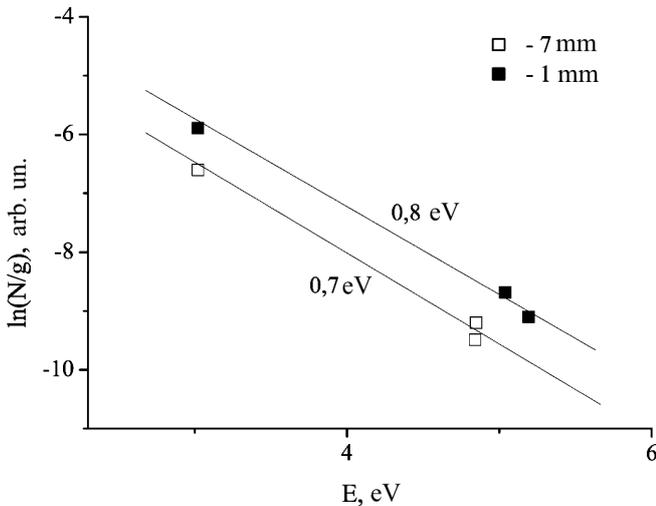
Fig. 4. Electron temperature in the CuInSe$_2$ laser plasma determined based on the excited-state population distribution of indium atoms

which the best values of photoelectric conversion are obtained.

The main reasons for the appearance of the first maximum at the oscillograms of radiation of the laser plasma are the atomization and the excitation of target atoms. The second maximum is caused by thermal processes taking place during the spread of the leading edge of the plasma to the surrounding gas, as well as the interaction of moving plasma particles with its atoms.

The laser radiation power is sufficient for the atomization of the target. Therefore, the laser plasma can contain Cu–Se, In–Se, and Cu–In–Se complexes, whose decay in various regions of the plasma in various time-space intervals also can result in the formation of excited atoms and ions. This fact is particularly confirmed by the formation of ions in a narrow interval of excited-state energies and the short time of observation of chalcogen atoms or ions as compared with other plasma components.

The electron concentration at a distance of 1 mm from the target in the CuInSe$_2$-based laser plasma amounts to 2.8×10^{16} cm^{-3}, which is higher than that in the corresponding compound with sulfur (2.2×10^{16} cm^{-3} [13]). This is mainly due to the differences in the atomization energies of these compounds and the smaller ionization energy of selenium atoms, as it is known that the breaking energy of bonds with sulfur is higher than that of bonds with selenium, which also has an effect on the energy gap width of selenide and sulphide compounds.

4. Conclusions

The most intense spectral lines radiated by the CuInSe$_2$-based laser torch plasma belong to indium and copper atoms (271.0, 293.3, 303.9, 410.2, and 451.1 nm In I and 324.8, 327.4, 521.8 nm Cu I). The oscillograms of the radiation intensity of the spectral lines have two maxima: one of then is most pronounced for transitions from highly excited atomic states, while the other one – for transitions from low-energy levels. The average velocities of the first maximum amount to 83 and 63 km/s for indium and copper plasma components, respectively, whereas those of the second maximum are equal to 14 and 12 km/s, respectively. The recombination time for singly charged indium ions is equal to 30 ns at an observation time of 25-50 ns and 56 ns at an observation time of ≈ 200 ns. The recombination time of the corresponding copper ions amounts to 139 ns for the time interval 250–300 ns. The laser torch plasma is characterized by the dominance of the recombination processes of formation of excited particles at the leading edge and the gradual transition to the prevalence of the excitation due to collisions with free electrons at the trailing edge. The electron temperature changes insignificantly (from 0.7 to 0.8 eV) as the distance grows from 1 to 7 mm. The temperature rise accompanying the plasma expansion is induced by the effect of the expansion gas dynamics on the plasma parameters: at close distances, plasma expands, while at large ones – it will be gradually compressed due to the accumulation of particles in a vicinity of the shock wave front. The electron concentration at a distance of 1 mm from the target in the CuInSe$_2$-based laser plasma amounts to 2.8×10^{16} cm^{-3}. The study of the parameters and the space characteristics of plasma provides the necessary information on its energy and component composition, which is determinative of the formation of thin films of the working elements of photoelectric converters with required structure and stoichiometry.

1. I.V. Bodnar and V.F. Gremenok, Zh. Prikl. Spektr. **74**, 90 (2007).

2. A.G. Guseinov, V.I. Tagirov, Z. Khosin, D. Dzhamel', and D.A. Talybova, VINITI **9**, 141 (1990).

3. Ya. Vertsimakha, P. Lutsuk, O. Lytvyn, and P. Gashin, Ukr. Fiz. Zh. **52**, 399 (2007).

4. A. Rose, *Concepts in Photoconductivity and Allied Problems* (Wiley, New York, 1963).

5. E.P. Zaretskaya, I.D. Viktorov, V.F. Gremenok, and D.V. Mudryi, Pis'ma Zh. Tekhn. Fiz. **27**, 17 (2001).

6. A.G. Guseinov, D.A. Talybova, Z. Khosin, and D. Dzhamel', VINITI, No. 1472-Az, 6 (1991).

7. O. Aissaoui, S. Mehdaoui, L. Bechiri, M. Benabdeslem, N. Benslim, A. Amara, L. Mahdjoubi, and G. Nouet, J. Phys. D: Appl. Phys. **40**, 5663 (2007).

8. I.V. Bodnar, V.F. Gremenok, Yu.L. Nikolaev, V.Yu. Rud', Yu.V. Rud', and E.I. Terukov, Pis'ma Zh. Tekhn. Fiz. **33**, 32 (2007).

9. P.L. Smith, C. Heise, J.R. Esmond, and R.L. Kurucz, *Atomic spectral line database from CD-ROM 23 of R.L. Kurucz* (Smithsonian Astrophys. Observ., Cambridge, 1995). http://cfa-www.harvard.edu/amp.

10. M.P. Chuchman and A.K. Shuaibov, Ukr. Fiz. Zh. **53**, 772 (2008).

11. M.P. Chuchman, A.K. Shuaibov, and G.E. Laslov, Pis'ma Zh. Tekhn. Fiz. **35**, 51 (2009).

12. L.L. Shimon, Ya.M. Semenyuk, and A.I. Dashchenko, *Plasma Physics* (Goverla, Uzhgotod, 2009) (in Ukrainian).

13. O.K. Shuaibov, M.P. Chuchman, L.L. Shimon, and I.E. Kacher, Ukr. Fiz. Zh. **48**, 223 (2003).

ЕМІСІЙНІ ХАРАКТЕРИСТИКИ ТА ПАРАМЕТРИ ПЛАЗМИ ЛАЗЕРНОГО ФАКЕЛА НА ОСНОВІ ПОЛІКРИСТАЛА CuInSe$_2$

М.П. Чучман, Г.Е. Ласлов, А.К. Шуаібов, Л.Л. Шимон

Р е з ю м е

Отримано спектри випромінювання та осцилограми інтенсивності спектральних ліній лазерної ерозійної плазми на основі сполуки CuInSe$_2$. Встановлено, що спектри випромінювання з гарячої зони цієї лазерної ерозійної плазми включають спектральні лінії збуджених атомів міді, індію, селену і їх однозарядних іонів. Визначено основні параметри та характеристики лазерного факела на основі сполуки CuInSe$_2$: швидкість поширення, часи рекомбінації іонів, температуру та концентрацію частинок. Показано, що на початкових етапах існування плазми основним процесом виступає рекомбінація, а при збільшенні відстані від мішені та часу затримки починають проявлятися газодинамічні та теплові ефекти, які значно визначатимуть особливості формування атомів та іонів у збуджених станах.